

CERN-TH/99-44
hep-ph/9902455

Pion Fluctuations near the QCD Critical Point

N.G. Antoniou^{a,b} ¹, Y.F. Contoyiannis^b and F.K. Diakonou^b

^a *Theory Division, CERN, CH-1211 Geneva 23, Switzerland*

^b *Department of Physics, University of Athens, GR-15771, Athens, Greece*

Abstract

A critical point of second order, belonging to the universality class of the 3d Ising model, has recently been advocated as a strong candidate for the critical behaviour (at high temperatures) of QCD with non-zero quark masses. The implications of this conjecture are investigated in the multiparticle environment of high-energy collisions. A universal intermittency pattern of pion-density fluctuations is found, at the critical point, and its association to the critical exponents is discussed. A Monte Carlo simulation of critical events, in heavy-ion collisions, reveals the detailed structure of these fluctuations, suggesting a framework of (event-by-event) measurements in which the critical theory of QCD may become falsifiable.

¹e-mail address: nantonio@atlas.uoa.gr

The nature of the QCD critical behaviour, associated with chiral phase transition, has gradually been better understood, during the last few years, in terms of the number of flavours and the primordial mass spectrum of the light quarks. In an approximate world of two flavours (u, d) with zero quark masses ($m_u \approx m_d \approx 0$), the high-temperature QCD phase transition ($T_c \approx 150\text{MeV}$) is of second order [1–3]; it belongs to the $O(4)$ universality class of a $3d$ Heisenberg magnet [3] and the order parameter is associated with pion and sigma field condensates $\phi = (\vec{\pi}, \sigma)$. In a more realistic world with three flavours (u, d, s) and a finite mass (m_s) of the strange quark, the system develops a tricritical point (m_s^*, T_c) at which the transition changes from first ($m_s < m_s^*$) to second order ($m_s > m_s^*$) [2, 3]. In the real world, however, with non-zero quark masses ($m_u, m_d \neq 0$) the second-order branch disappears from the phase diagram: the corresponding transition becomes a smooth crossover [4] and the tricritical point is transformed into an endpoint of the first-order phase transition line (critical point of second order). It has also been argued [5, 6] that the behaviour of the system near the QCD critical point (T_c, μ_c) belongs to the universality class of the Ising model in $3d$ (gas–liquid transition); in this case, the order parameter is associated with the σ -field condensate alone, $\sigma \sim \langle \bar{\psi}\psi \rangle$. The above over-all picture of critical QCD has been advocated recently by a number of authors [3–8] and despite the fact that one cannot (yet) verify these ideas completely in a detailed *ab initio* study on the lattice, owing to the involvement of a non-zero chemical potential μ_c at the critical point, this picture remains attractive, as it is based on rather general and universal properties of strong interactions, near criticality. In this Letter we claim that it can also be falsifiable, because it may lead to quantitative and sharp predictions for pion-density fluctuations, near the critical point. Such critical fluctuations can, in principle, be measured in relativistic heavy-ion collisions, by selecting rare events with strong and universal intermittency pattern [9] in momentum space.

To this end, consider the $3d$ effective action $\Gamma_c[\sigma]$, which effectively describes the system of QCD at the critical point ($T = T_c, \mu = \mu_c$) :

$$\Gamma_c[\sigma] = T_c^{-1} \int d^3\vec{x} \left[\frac{1}{2}(\nabla\sigma)^2 + GT_c^4(T_c^{-1}\sigma)^{\delta+1} \right]. \quad (1)$$

In eq.(1) the macroscopic field σ has a dimension $\sigma \sim (\text{length})^{-1}$, δ is the isothermal critical exponent, and G , a dimensionless coupling, specifies the

critical equation of state: $\frac{\delta\Gamma_c}{\delta\phi} \sim G\phi^\delta$. Both parameters (G, δ) are universal; in the $3d$ Ising class one may fix the exponent at the mean field value $\delta \approx 5$, because of the smallness of the anomalous dimension [10]. The coupling G , for the same universality class, has been estimated recently, in non-perturbative studies of the critical equation of state, and its actual value is fixed, to a good approximation, in the range $G \approx 1.5\text{--}2.5$ [10]. Hence the only free parameter in the effective theory (1) is essentially the critical temperature T_c , which determines the length scale (in heavy-ion physics, $\beta_c = T_c^{-1} \sim 1\text{--}2$ fm).

In order to test the theory (1) in the environment of a high-energy collision, we have to first adapt the longitudinal geometry to the rapidity space (ξ) by introducing the proper time-scale (τ) of the collision $(A + A)$:

$$\Gamma_c[\sigma] = \frac{1}{C_A} \int d^2\vec{x}_\perp d\xi \left[\frac{1}{2} \left(\frac{\partial\sigma}{\partial\xi} \right)^2 + \frac{\tau^2}{2} (\nabla_\perp \sigma)^2 + GC_A^2 \beta_c^4 \sigma^6 \right], \quad (2)$$

where $C_A = \frac{\tau}{\beta_c}$. The effective field $\sigma(\xi, \vec{x}_\perp)$, being macroscopic (classical), is naturally associated with the density of σ -particles in the $3d$ space (ξ, \vec{x}_\perp) : $\sigma^2 = N_\sigma(\text{volume})^{-1} \sim (\text{length})^{-2}$. Technically, this interpretation follows from the requirement that the density matrix, associated with the partition function $Z = \int [\mathcal{D}\sigma] e^{-\Gamma_c}$ of the critical theory (2), be diagonal in the coherent-state representation of the particles associated with the σ -field [11]. As a consequence, one finds for the average multiplicity $\langle N_\sigma \rangle$ the form: $\langle N_\sigma \rangle = Z^{-1} \int [\mathcal{D}\sigma] e^{-\Gamma_c} (\int d^2\vec{x}_\perp d\xi \sigma^2(\xi, \vec{x}_\perp))$, suggesting that the appropriate order parameter for the study of the density fluctuations of the isoscalar particles at the critical point, is $\sigma^2(\xi, \vec{x}_\perp)$ [12].

In the cylindrical geometry of the collision, the theory (2) can be solved by projecting out the effective action onto rapidity and transverse space. Following the results in ref. [13], the critical fluctuations of the order parameter in these two spaces ($1d$ and $2d$) are developed within clusters of size $\delta_c = \frac{\pi^{1/2} R_\perp}{2\tau}$ and $r_{\perp c} = \frac{\pi^{3/2} R_\perp}{32}$ respectively (R_\perp is the transverse radius of the entire system at the critical point). These fluctuations are properly described (with the expected fractal dimension) by the contribution to the partition function of instanton-like configurations, which, within these clusters, are slowly varying functions and contribute equally to the effective potential and to the derivative terms in eq. (2) [13]. In this framework, the canonical partition function, at $T = T_c$, for scalar particles (σ) in a cylindrical volume

$V \leq \pi \delta_c r_{\perp c}^2$, is written:

$$Z(N_\sigma, V, T_c) = N_\sigma^{-1/2} \exp \left[- \left(\frac{V_o}{V} \right)^2 N_\sigma^3 \right], \quad (3)$$

where $V_o = \beta_c^2 \sqrt{2GC_A}$.

The average multiplicity $\langle N_\sigma \rangle$ of scalars, in each $3d$ cluster, as a function of the volume V , now follows from (3):

$$\langle N_\sigma \rangle = \frac{\Gamma(1/2)}{\Gamma(1/6)} \left(\frac{V}{V_o} \right)^{2/3} \quad ; \quad V \gg V_o. \quad (4)$$

Equation (4) shows that the critical clusters are local, cylindrical fractals with a minimal volume-scale $V = V_o$ where self-similarity breaks down. The fractal dimensions in rapidity and transverse space are $d_{F,1} = \frac{2}{3}$ and $d_{F,2} = \frac{4}{3}$, reflecting the actual value of the isothermal critical exponent $\delta \approx 5$ and also the choice of the order parameter σ^2 ($d_{F,1} = \frac{\delta-1}{\delta+1}$, $d_{F,2} = \frac{2(\delta-1)}{\delta+1}$). The corresponding density-density correlation function obeys for each cluster a characteristic power-law:

$$\langle \rho(\xi, \vec{x}_\perp) \rho(0, 0) \rangle = \left(\frac{32}{\pi GC_A} \right)^{1/3} \beta_c^{-2} \frac{\Gamma(1/2)}{\Gamma(1/6)} |\xi|^{-1/3} \left| \frac{\vec{x}_\perp}{\beta_c} \right|^{-2/3}. \quad (5)$$

Since the size of the critical clusters specifies also the correlation length of the finite system [13], both in rapidity ($\delta_c = \frac{\sqrt{\pi} R_\perp}{2\tau} \left(\frac{G}{2} \right)^{-1/2}$) and transverse space, ($r_{\perp,c} = \frac{\pi^{3/2}}{32} \left(\frac{G}{2} \right)^{-3/4} R_\perp$) we may safely assume that in the global volume $V_g = \pi R_\perp^2 \Delta$ (Δ is the total rapidity available in the experiment) the critical clusters interact weakly, so that they form an ideal classical gas with a Poisson multiplicity distribution [14]. The average multiplicity of clusters, in this approximation, is $\langle N_{cl} \rangle \approx \left(\frac{R_\perp}{r_{\perp,c}} \right)^2 \left(\frac{\Delta}{\delta_c} \right)$ and, using eq. (4), an upper bound of the excess multiplicity of pions produced when the system passes through the critical point, can be extracted ($N_\pi \approx 2N_\sigma$) $\frac{N_\pi}{\Delta} \leq \frac{16}{\sqrt{\pi}} \left(\frac{R_\perp}{\beta_c} \right) \left(\frac{G}{2} \right)^{7/12}$. On the other hand, the local fractals, associated with the critical clusters finally build-up a global fractal with the same dimension [15]. In fact, in the transverse momentum space, the fractal \tilde{F}_2 is even stronger, since the corresponding Fourier transform of the power-law (5) gives $\tilde{d}_{F,2} = \frac{2}{3}$ ($\tilde{d}_{F,2} = 2 - d_{F,2}$). On the basis of these structures, the theory predicts a universal

pattern of strong, multidimensional intermittency (in rapidity, transverse momentum and $3d$ momentum space) of the form: $F_p^{(1)} \sim M^{\frac{p-1}{3}}$, $F_p^{(2)} \sim (M^2)^{\frac{2(p-1)}{3}}$, $F_p^{(3)} \sim (M^3)^{\frac{5(p-1)}{9}}$ ($p = 2, 3, \dots$) where F_p is a scaled factorial moment of order p [9] as a function of M , the number of one-dimensional cells in momentum space. Other power-laws coming from the $1d$ projections of the fractal \tilde{F}_2 or from the Cartesian product of two fractals in the cylindrical geometry of the system, can also be written [12]. The predicted intermittency power-laws describe the density fluctuations of scalars produced at the critical point quantitatively, relating these fluctuations to the critical exponents of the $3d$ universality class.

We have performed a Monte Carlo simulation of the critical events in Pb+Pb collisions in the SPS ($\Delta \approx 6$), corresponding to the choice of the parameters: $T_c = 120$ MeV, $R_\perp = 30$ fm, $\tau_c = 25$ fm. We have also fixed the coupling G at the value $G = 2$ [10]. In momentum space, the isoscalar particles (σ) are grouped in critical clusters (cylindrical) with appropriate power-law correlations, dictated by the Fourier transform of eq. (5) in transverse space: $\langle \tilde{\rho}(\xi, \vec{p}_\perp) \tilde{\rho}(0, 0) \rangle \sim |\xi|^{-1/3} |\beta_c \vec{p}_\perp|^{-4/3}$. The distribution of the clusters in rapidity (projected) corresponds to an ideal $1d$ gas, whereas in transverse momentum space the following extra constraints are imposed: (a) the clusters (their centers) are exponentially distributed according to the temperature T_c , $dn_c \sim \exp(-\frac{p_{\perp,c}}{T_c})$ and (b) the total transverse momentum carried by the clusters is zero, $\sum_i \vec{p}_{\perp,c}^{(i)} = 0$. Moreover the size of the critical clusters in transverse momentum space, as determined by the minimum length scale in transverse configuration space, is given by the expression $|\Delta \vec{p}_\perp| \approx \frac{T_c}{2} \left(\frac{R_\perp}{\tau_c} \right)^{1/2} \left(\frac{G}{2} \right)^{-3/8} \left(\frac{\pi^3}{c_A} \right)^{1/4}$ and for the above set of parameters we estimate $|\Delta \vec{p}_\perp| \approx 70$ MeV. With these ingredients and the overall constraints on the formation of sigmas at $T = T_c$, a typical, simulated event is obtained with characteristics shown in Figs.1–3: the overall picture is consistent with a $3d$ cylindrical fractal in momentum space (Fig. 1), which is decomposed into a $2d$ self-similar structure in transverse momentum space (Fig. 2) and a $1d$ self-similar structure in rapidity space (Fig. 3). The multidimensional intermittency pattern clearly reveals a linear spectrum of indices in each case, consistent with the critical exponents of the theory [13].

In the process of a phase transition in thermal equilibrium, the fluctuating system is very likely to get frozen immediately after crossing the critical

point of second order (μ_c, T_c) [7]; therefore, the fluctuations predicted at $T = T_c$ may enter the horizon of observation (in the corresponding events) without any distortion ($T_f \approx T_c$). It remains to guarantee that the decay of σ may proceed near the $\pi\pi$ threshold, rather rapidly transferring the critical fluctuations found at $T = T_c$ automatically to the π^- spectra ($\sigma \rightarrow \pi^+\pi^-$) (Figs. 1–3). The isoscalar σ has a very small mass at $T = T_f$; therefore, the system of sigmas remains frozen and stable until the mass m_σ , as a function of temperature, rises to the $\pi\pi$ threshold value, $m_\sigma = 2m_\pi$. If the corresponding time scale τ_{th} is sufficiently long (in particular events), the expansion rate $|\frac{\dot{T}}{T}| \leq \frac{1}{3\tau_{th}}$, for $\tau \geq \tau_{th}$, becomes very small with respect to the decay rate of σ (even near the $\pi\pi$ threshold), also because the isoscalar is very strongly coupled to the $\pi\pi$ system. Under these circumstances, the sigmas with $m_\sigma \gtrsim 2m_\pi$ have enough time to decay, before their mass increases further, leading to charged pions (π^-) with the same fluctuation pattern in momentum space. We have verified numerically this decay mechanism, near the $\pi\pi$ threshold, in the case of the typical event shown in Figs. 1–3. We have used for the parameters of the σ -meson in vacuum ($T = 0$) the average values $m_\sigma^{(0)} \approx \Gamma_\sigma^{(0)} \approx 0.8$ GeV of the $f_o(400 - 1200)$ $\pi\pi$ resonance [16]. It turns out that, if $\tau_{th} \gg 10$ fm, the decay $\sigma \rightarrow \pi\pi$ proceeds near $\pi\pi$ threshold and therefore the intermittency pattern found at $T = T_c$ for sigmas (Figs. 1–3) is also a prediction for the density fluctuations of the abundant charged pions (π^-) associated with the critical point.

In the framework of heavy-ion physics, we have derived a pattern of local dynamical fluctuations of the classical σ -field associated with the critical point in QCD with non-zero quark masses. This critical point belongs to the $3d$ Ising universality class, but the same pattern is valid in any universality class associated with a $3d$ scalar theory. The reason is that, in these theories, the anomalous dimension η is very small [10], leading to the same (mean field) value of the exponent: $\delta \approx 5$. Hence a similar pattern of fluctuations is expected, for instance, in the $O(4)$ $3d$ theory [14], which describes the chiral QCD phase transition in the limit of zero quark masses [3]. At the level of observed pions, however, these theories are expected to lead to different fluctuation patterns since the in-medium evolution (and decay) of scalars varies from one universality class to the other. In the case of real QCD with non-zero quark masses, we have argued that in a particular class of events, in which the in-medium evolution of σ is rather slow, $\tau_{th} \gg \tau_c$,

the fluctuation pattern found at $T = T_c$ (Figs. 1–3) is inherited by the charged decay products of σ near the $\pi\pi$ threshold (π^-) and manifests itself as a clear signature of the quark-hadron phase transition in nuclear collisions.

We thank A.L.S. Angelis and C.G. Papadopoulos for their comments and suggestions on the present work.

References

- [1] R. Pisarski and F. Wilczek, Phys. Rev. **D29**, 338 (1984).
- [2] Columbia Group, Phys. Rev. Lett. **65**, 2491 (1990).
- [3] F. Wilczek, Int. J. Mod. Phys. **A7**, 3911 (1992);
K. Rajagopal and F. Wilczek, Nucl. Phys. **B399**, 395 (1993).
- [4] J. Berges, D.-V. Jungnickel and C. Wetterich, hep-ph/9705474.
- [5] J. Berges and K. Rajagopal, hep-ph/9804233.
- [6] M. A. Halasz, A. D. Jackson, R. E. Shrock, M. A. Stephanov and J. J. M. Verbaarschot, Phys. Rev. **D58**, 096007 (1998).
- [7] M. A. Stephanov, K. Rajagopal and E. Shuryak, Phys. Rev. Lett. **81**, 4816 (1998).
- [8] F. Wilczek, Nature **395**, 220-221 (1998).
- [9] A. Bialas and R. Peschanski, Nucl. Phys. **B273**, 703 (1986); **B308**, 857 (1988).
- [10] M. M. Tsypin, Phys. Rev. Lett. **73**, 2015 (1994); J. Berges, N. Tetradis and C. Wetterich, Phys. Rev. Lett. **77**, 873 (1996).
- [11] J. C. Botke, D. J. Scalapino and R. L. Sugar, Phys. Rev. **D9**, 813 (1974).
- [12] N. G. Antoniou, C. N. Ktorides, I. S. Mistakidis and F. K. Diakonou, Eur. Phys. J. **C4**, 513 (1998).

- [13] N. G. Antoniou, Y. F. Contoyiannis, F. K. Diakonou and C. G. Papadopoulos, Phys. Rev. Lett. **81**, 4289 (1998).
- [14] N. G. Antoniou, F. K. Diakonou, C. N. Ktorides and M. Lahanas, Phys. Lett. **B432**, 8 (1998).
- [15] A. Lesne, “*Renormalization Methods: Critical Phenomena, Chaos, Fractal Structures*”, (John Wiley and Sons Ltd., Chichester, 1998).
- [16] Meson Particle Listings, Eur. Phys. J. **C3**, 363 (1998).

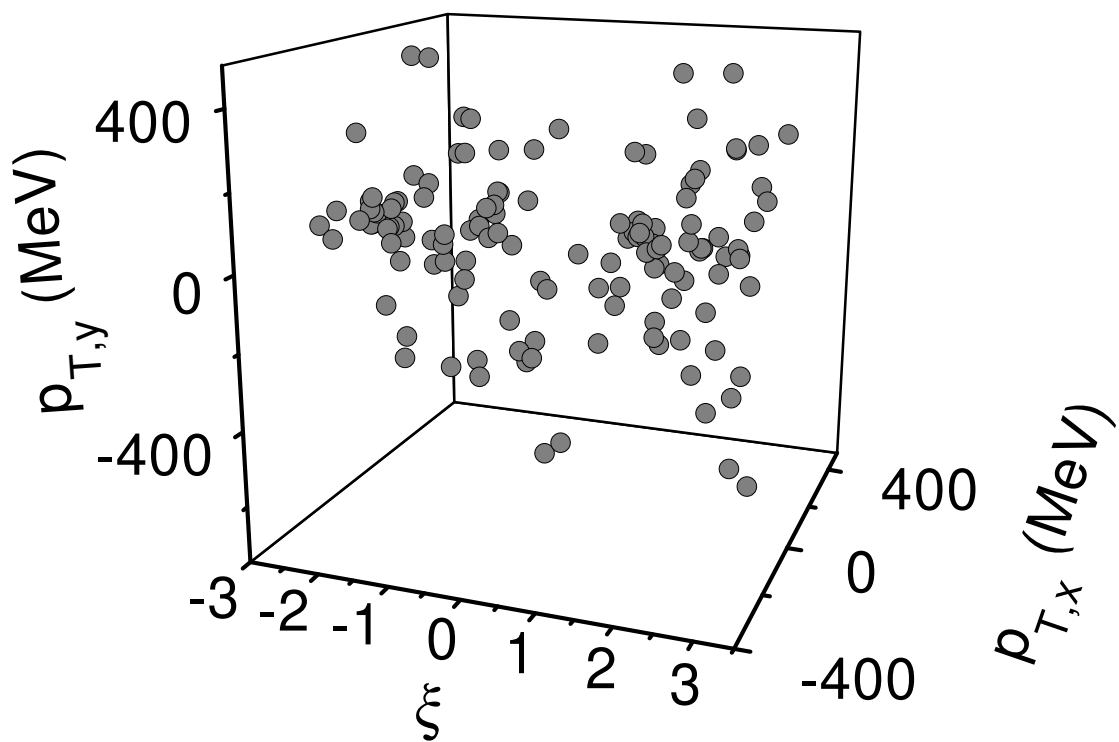
Figure Captions

Figure 1: (a) The distribution of the σ -particles of a typical critical event in $3d$ momentum space. The multiplicity of σ 's is 138. (b) The corresponding $(3d)$ factorial moments of order $p = 2, 3, 4$ in a log-log plot. A linear fit (dashed line) indicating the intermittency pattern for this event is included.

Figure 2: (a) The distribution of the σ -particles in transverse-momentum space for the event of Fig. 1. (b) The corresponding $(2d)$ factorial moments of order $p = 2, 3, 4$ in a log-log plot. A linear fit (dashed line) indicating the resulting intermittency pattern is also shown.

Figure 3: (a) The distribution of the σ -particles in rapidity for the event of Fig. 1. (b) The rapidity factorial moments of order $p = 2, 3, 4$ in a log-log plot together with a linear fit (dashed line) indicating the corresponding intermittency pattern.

(a)



(b)

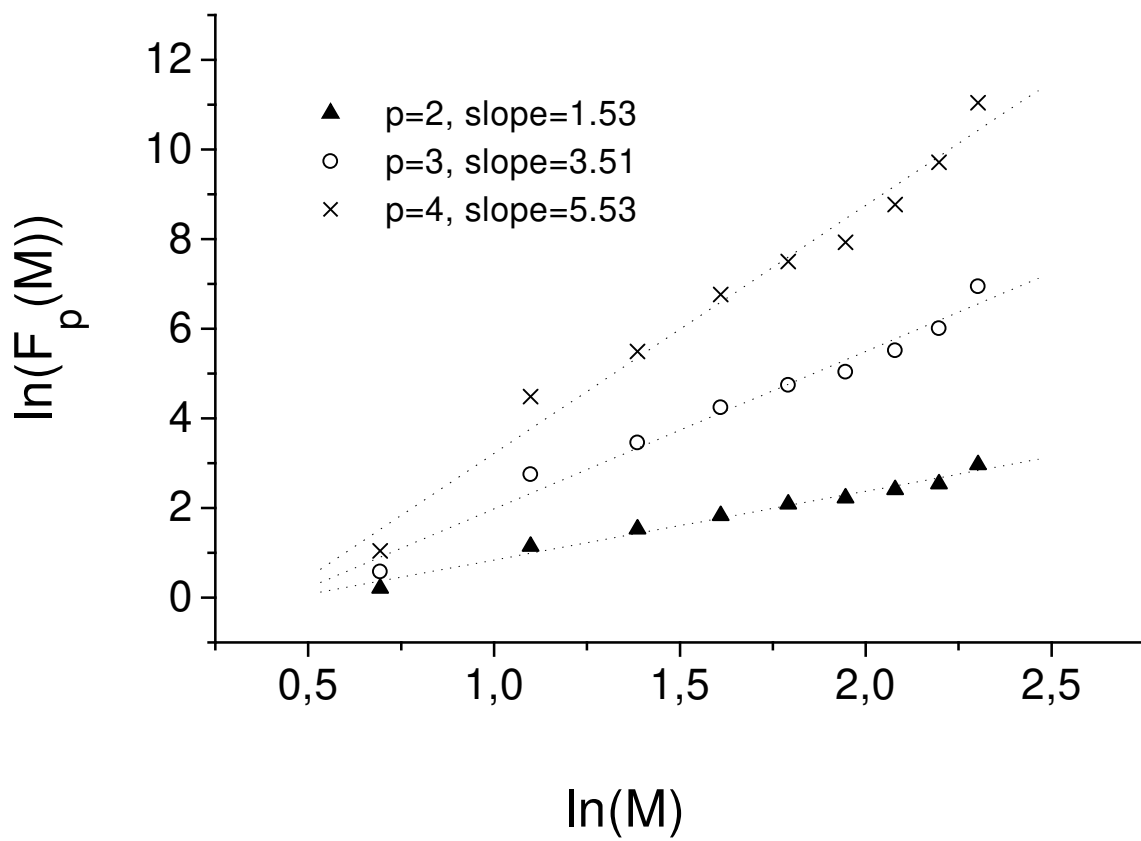


Figure 1

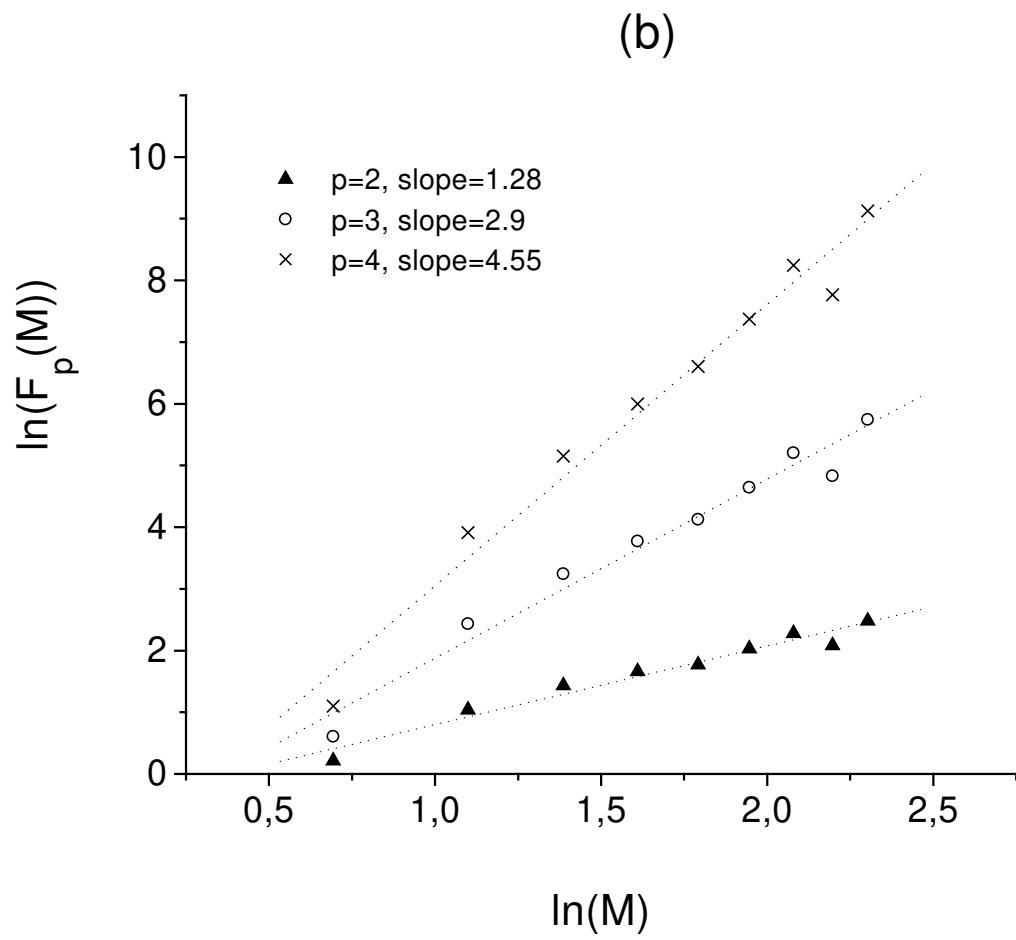
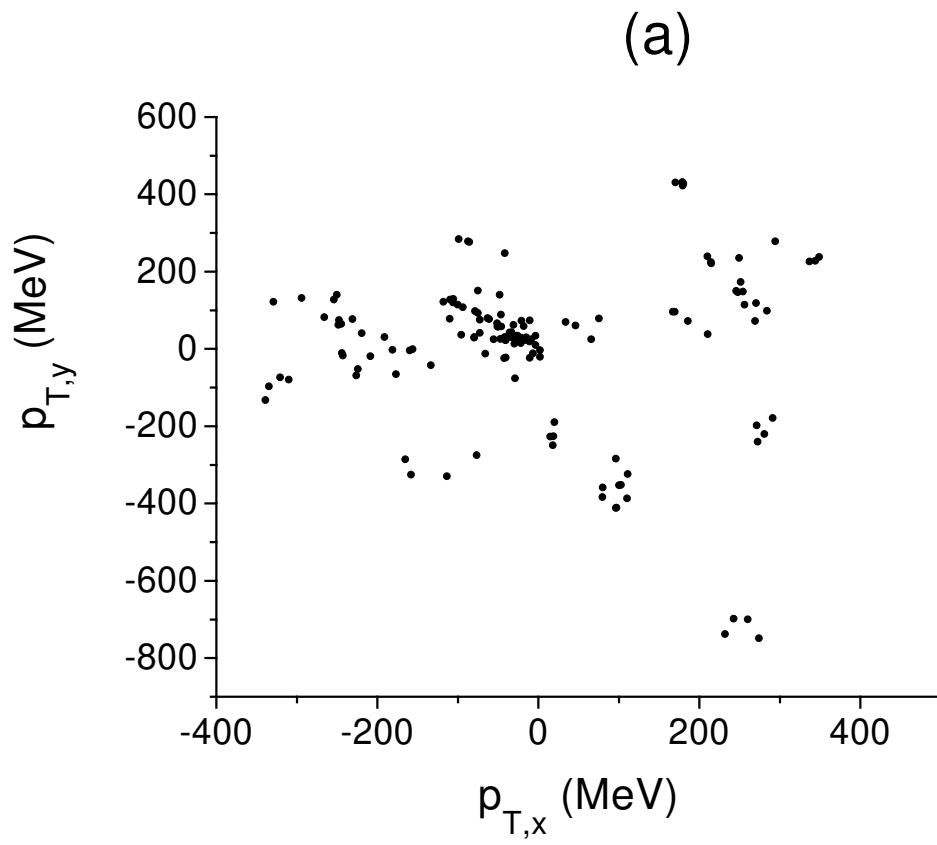


Figure 2

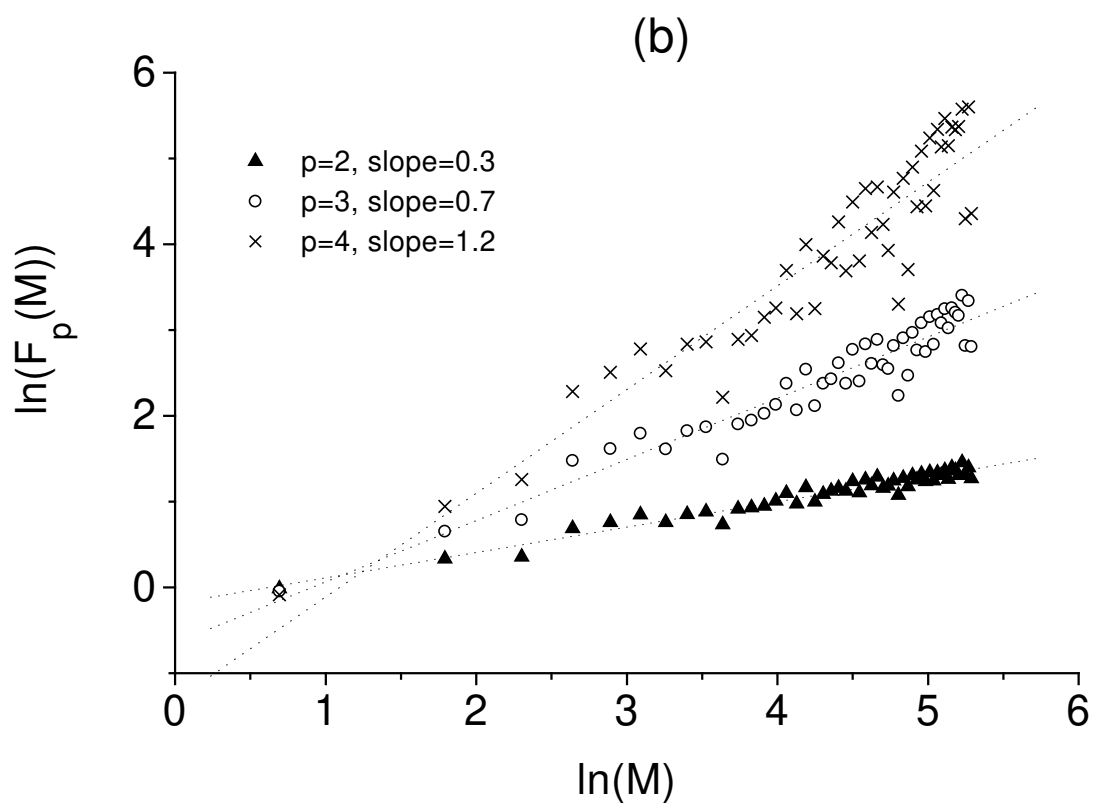
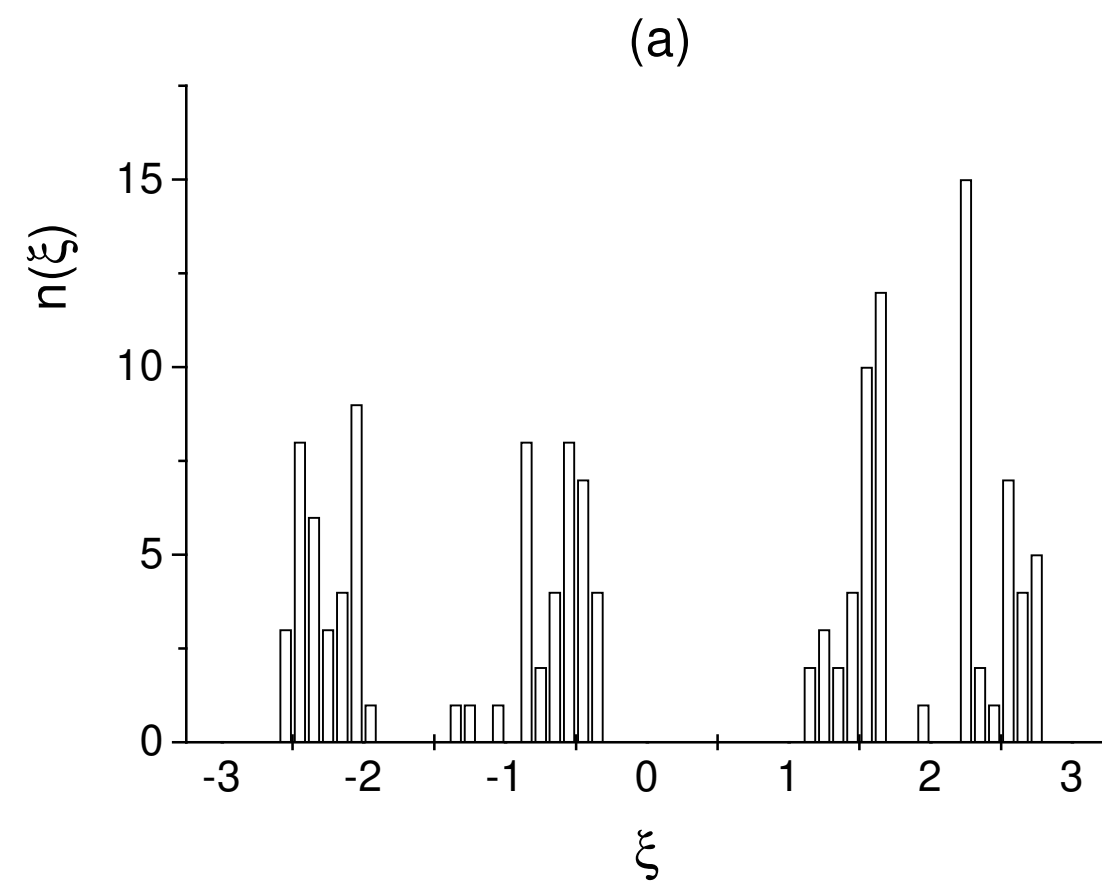


Figure 3

